

The Design and Mathematical Model of a Novel Variable Stiffness Extensor-Contractor Pneumatic Artificial Muscle (ECPAM)

Hassanin Al-Fahaam*, Samia Nefti-Meziani, Theo Theodoridis and Steve Davis

Abstract

This article presents the design of a novel Extensor-Contractor Pneumatic Artificial Muscle (ECPAM). This new actuator has numerous advantages over traditional pneumatic artificial muscles. These include the ability to both contract and extend relative to a nominal initial length, the ability to generate both contraction and extension forces and the ability to vary stiffness at any actuator length. A kinematic analysis of the ECPAM is presented in this article. A new output force mathematical model has been developed for the ECPAM based on its kinematic analysis and the theory of energy conservation. The correlation between experimental results and the new mathematical model has been investigated and show good correlation. Numerous stiffness experiments have been conducted to validate the variable stiffness ability of the actuator at a series of specific fixed lengths. This has proven that actuator stiffness can be adjusted independently of actuator length. Finally a stiffness-position controller has been developed to validate the effectiveness of the novel actuator.

Keywords: soft robotics, soft mechanisms, soft actuators, pneumatic artificial muscles, modelling, variable stiffness.

1. Introduction

An assortment of creatures and plants perform complicated movements using soft structures that do not have rigid parts. Muscular hydrostats such as the arms of an octopus and the trunk of an elephant are almost totally composed of muscles and connective tissue; plant cells are also capable of changing their shape through osmosis without the need for a rigid skeletal structure. Scientists have been inspired by these creatures and plants to design and manufacture robots that use artificial soft actuators which do not have rigid skeletons. These robots are commonly referred to as soft robots.

These soft robots typically have high numbers of degrees of freedom and are able to flex and bend at multiple locations rather than at discrete fixed joint locations as is the case for a traditional robot. This means soft robots can deform when they are in contact with an object, distributing contact stresses over a greater area. This, combined with the fact that many soft robots are constructed from lightweight materials, means soft robots are potentially safer for human interaction than traditional robots. Figure 1 shows examples of muscular hydrostats and hydroskeletons. These creatures are typically capable of moving without skeletal support [1].

Soft robots often use soft and compliant actuator and one of the most well known soft actuator is the pneumatic artificial muscle (PAM). Pneumatic artificial muscles vary significantly from conventional pneumatic actuators and have seen application in bionic, anthropomorphic and humanoid robots, physiotherapeutic and rehabilitation robots, and also for the mechanization of industrial processes. Pneumatic artificial muscles are lightweight, soft and single-acting [2-7].



Figure 1. Examples of muscular hydrostats and hydroskeletons.

One of the major drivers for researchers to develop and use pneumatic muscles is the performance similarity between them and organic muscles [8-10]. Tsagarakis and Caldwell [11] analysed these similarities as illustrated in Table 1. The most common pneumatic muscle design is based on the McKibben muscle. Pneumatic artificial muscles have been used in many biologically inspired robots as well as in soft robots such as continuum robots [6, 12-16]. As pneumatic muscles are constructed from soft materials, they have the capability to provide much safer interaction with humans than is possible with traditional rigid robots and actuators [17, 18].

Table 1. Comparison of pneumatic artificial muscles and natural muscles.

Parameter	Organic Muscle	PAM
Displacement	35%	30-68%
Force/cm ²	20-40 N	100-500 N
Power/Weight	40-250 W/Kg	500-2000 W/kg
Efficiency	45-70%	32-50%
Control	Good	Fair-Good
Operation in Water	Yes	Yes
Temperature Range	0-40° C	-30-80°C
Robustness	Excellent	Fair-Good
Energy Source	Chemical	Pneumatic
Environment Safe	Produces CO ₂	Yes
Scalable from	µm-m	cm-m

A pneumatic muscle consists of an internal elastomeric bladder surrounded by a woven braided shell. As the actuator is pressurised it experiences a linear change in length. Depending upon how the muscle is constructed it will either contract when pressurised (contractor muscle) or extend (extensor muscle). No single muscle is capable of both types of motion and contractor muscles have undergone considerably more research than extensor muscles. Zheng and Shen [19] explored the development of a bi-directional pneumatic muscle by including a rigid pneumatic cylinder inside a soft pneumatic muscle. Although this approach allowed the actuator to create force in both directions the inclusion of the pneumatic cylinder means the actuator is neither soft nor lightweight. Hassan, et al. [20] presented a multifunctional pneumatic muscle capable of generating bi-directional force. The system allowed the resting braid angle of the actuator to be adjusted mechanically. This meant that the actuator could be adjusted to produce either a contractile force or an expansive force. The system however, was not capable of producing bi-directional force without mechanical adjustment of the actuator.

Daerden and Lefeber [21] illustrate the most important properties of PAMs as follows:

Static load characteristics: under static conditions, the PAM equilibrium length will be determined by the pressure, the external load and the volume to length ratio of that specific muscle.

Compliance: As a result of air compressibility, every pneumatic actuator demonstrates compliant behaviour. Regardless of the fact that the pressure is kept at a fixed value, the muscle demonstrates spring-like behaviour because of the change of force with respect to length.

Antagonistic set-up: Pneumatic muscles are contraction devices, and can produce movement in one direction only, like real muscles. To generate bidirectional movements, two muscles are needed, one for each direction. One actuator moves the load in one direction and the other one works as a brake to reach the desired position; changing the muscles' operation produces an opposite movement.

Skeletal Muscle Resemblance: PAMs are similar to skeletal muscle in functional behaviour, in that both use linear contraction motion with a monotonical relation between decreasing load and the contractile ratio (which does not always happen in real skeletal muscles). To produce bidirectional movement, both require an antagonistic set-up to be able to control the joints efficiently.

Lightweight and strong: PAMs are extremely lightweight because their components are soft and small. Output force for these actuators is extremely high, up to several thousand Newtons.

Ready replacement: Replacement of a damaged PAM is extremely easy and rapid.

Hazard-free use: pneumatic actuators use air pressure, resulting in no pollution, and the soft materials are also safer than rigid units. As a result, pneumatic soft actuators are safer for human interaction than many rigid actuation systems.

There have been numerous attempts to model the behaviour of PAMs [22]. However, there is currently no 100% accurate mathematical model for these actuators, because of their highly nonlinear behaviour, and the materials they are constructed from (latex or rubber) they also show high levels of hysteresis. Most previous models have concentrated on contracting PAMs and there is a lack of models for extensor PAMs and bending muscles [23]. Many methods have been used to create efficient controllers for these soft pneumatic actuators, but this is hindered by the lack of accurate mathematical models.

There have been numerous applications of PAMs demonstrated over the last 20 or so years, covering many fields such as biorobotic, medical, industrial, and aerospace applications [24].

Recently, there has been a considerable amount of research into the mathematical modelling of contraction PAMs. The purpose is to create a mathematical relationship between the length of the PAM, the amount of pressure inside it, and the force it generates. These mathematical models depend on variable parameters such as applied pressure, axial force, length and diameter of the PAMs, as well as the properties of the materials used. All these variables play a considerable role in the dynamic behaviour of the soft actuators. There is strong evidence of the non-linear behaviour of PAMs; thus, the major challenge is to build a robust controller for this [25, 26]. A classification of the most common and promising mathematical models of pneumatic muscles was made by Tondu [23].

This paper reports the development of a novel Extensor-Contractor pneumatic artificial muscle. The main contributions of the new actuator are its capability to both contract and extend relative to its resting length with both contraction and extension forces being generated. The new actuator also allows the muscle's stiffness to be varied at any specific length. The design and construction of this actuator are explained in detail below. A new output force mathematical model for the novel actuator is presented. This mathematical model has been validated experimentally. Stiffness and position control experiments have been performed to validate the main contribution of the new actuator.

2. Contraction Pneumatic Artificial Muscles

The new actuator developed in this work uses a combination of both contractor and extensor pneumatic muscles. The behaviour of these two muscle types will be investigated before they are combined into a single actuator.

The contractor muscles used in this research are constructed from a braided nylon sleeve with a maximum unpressurised extended length of 18.4cm and a corresponding resting diameter of 5mm; an inner bladder formed from two layers of latex rubber tube 18.4cm length and 5mm diameter and two 3D printed cap ends, one which

is closed and the other with a port through which compressed air can be supplied to the muscle. A contraction muscle decreases in length when the applied pressure is increased until it reaches its minimum energy state, which occurs at a braid interweave angle of 54.7° .

The characteristic relation between the supplied air pressure and the actuator contraction was explored. The contraction occurs when increasing the supplied pressure, and this results in the creation of a contractile force. The maximum contraction ratio of the actuator used is approximately 30% at 500kPa pressure.

The stiffness of a PAM is proportional to the pneumatic pressure within it [27]. An experiment was performed to calculate the stiffness of the contractor actuator at a range of different applied pressures. Figure 2 shows the experimental setup used. The actuator was positioned vertically with the muscle end cap through which air is applied secured to a fixed mounting plate. The unloaded muscle was then pressurised and its contracted length was recorded. Increasing loads were then applied to the free end of the muscle and the resulting change in length of the muscle at each load value was recorded. This experiment was repeated four times with four supplied pressures (200kPa, 300kPa, 400kPa and 500kPa). Figure 3 demonstrates the results of these four experiments and Figure 4 shows the behaviour of the contraction muscle stiffness as the applied pressure is increased.

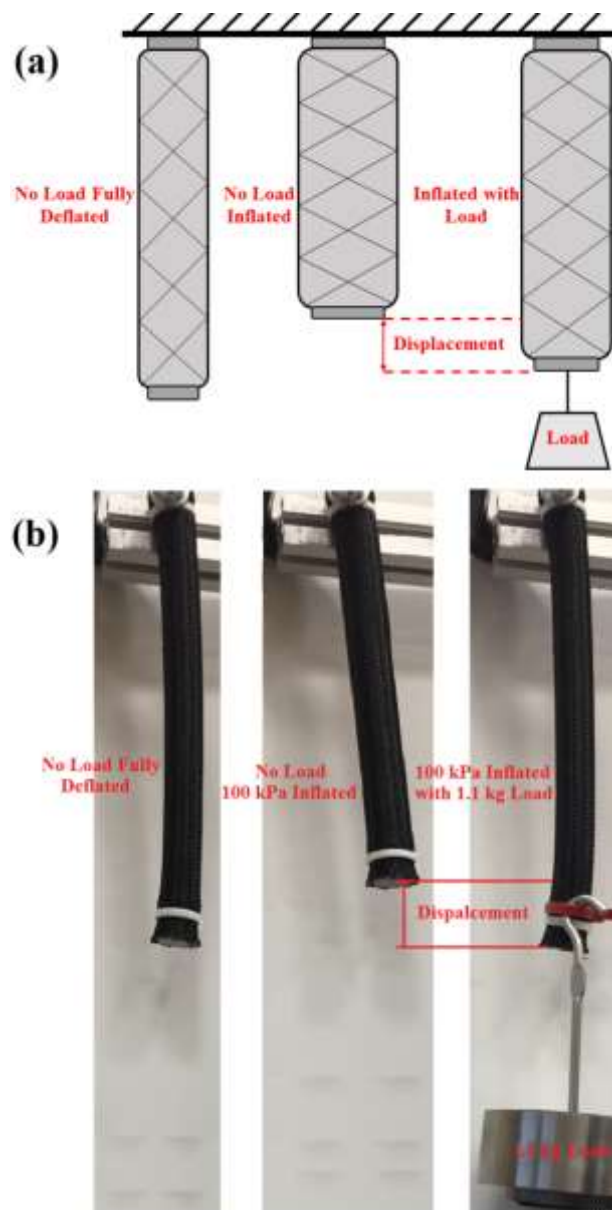


Figure 2. Experiment setup to calculate the stiffness of the PAM; (a) Experiment schematic description and (b) The real experiment.

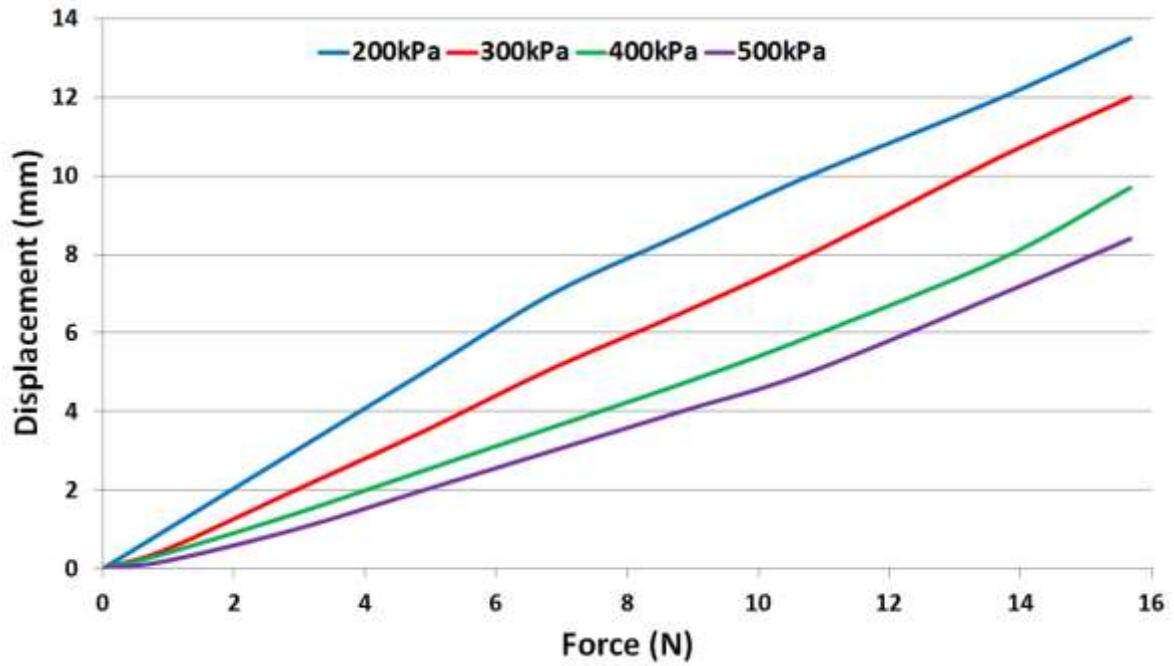


Figure 3. The experimental results of the contraction muscle change in length with different attached loads at specific amounts of supplied pressure.

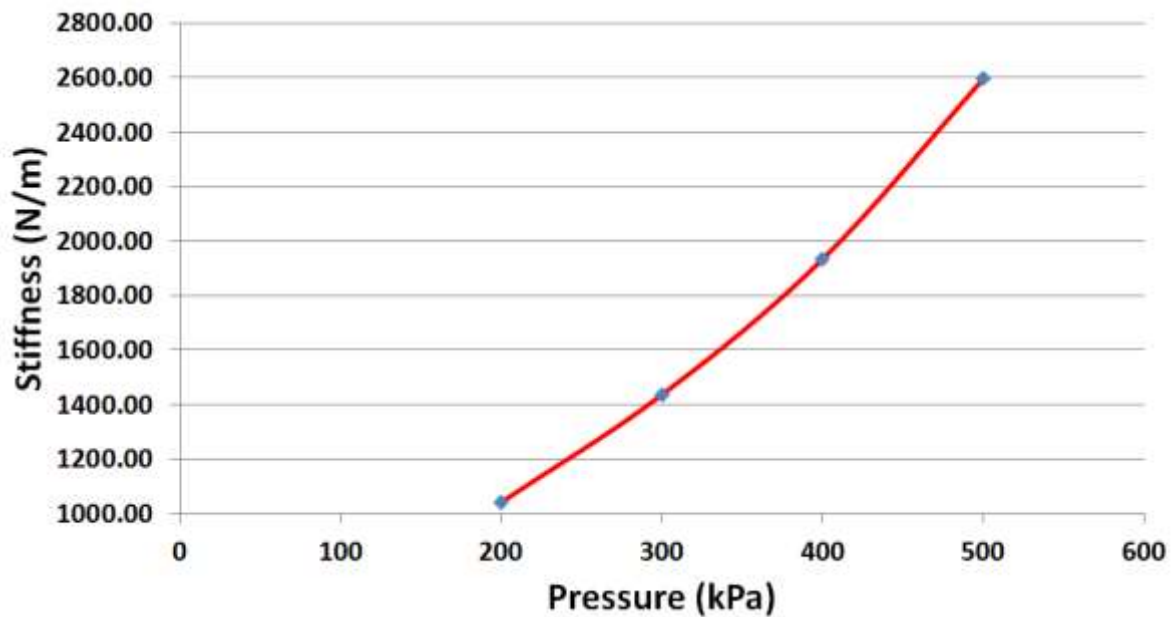


Figure 4. The contraction muscle stiffness in relation with increasing the supplied pressure.

3. Extensor Pneumatic Artificial Muscles

The extensor artificial muscle used in the development of the new actuator uses the same type of woven braid as for the contractor muscle. However, the resting diameter of the braid was double that of the contractor muscle (10mm) and its length was 32cm. The inner rubber tube of the extensor muscle also had a diameter of 10mm and was half the length of the braided sleeve (16cm). The muscle end caps were the same as those used with the contractor muscles. As the braided sleeve was considerably longer than the length of the rubber tube it needed to be compressed axially to match the length of the bladder. This meant that the muscle had a resting braid interweave angle greater than 54.7° which meant when it was pressurised the muscle would extend in length.

The relationship between the pressure inside the muscle and muscle length when no load is applied was investigated experimentally. It was found that the extensor muscle achieves a maximum length of 25.1cm at 500kPa pressure. This represents an extension from its resting, unpressurised, length of 56%.

To calculate the stiffness of the extensor muscle, the same experiment used to determine the stiffness of the contraction muscle was performed. This experiment was also repeated four times with four supplied air pressures (100kPa, 200kPa, 300kPa and 400kPa). Figure 5 illustrates the results of these four experiments and Figure 6 shows the behaviour of the extensor muscle stiffness when increasing the supplied air pressure.

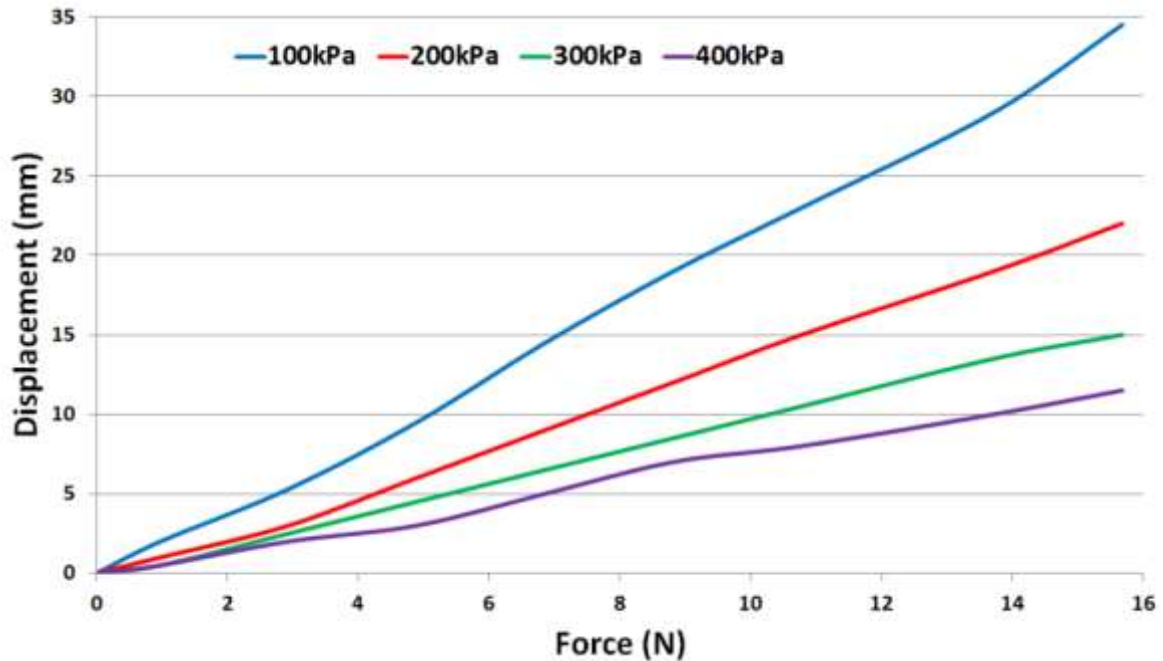


Figure 5. The experimental results of the contraction muscle change in length with different attached loads at specific amounts of supplied pressure.

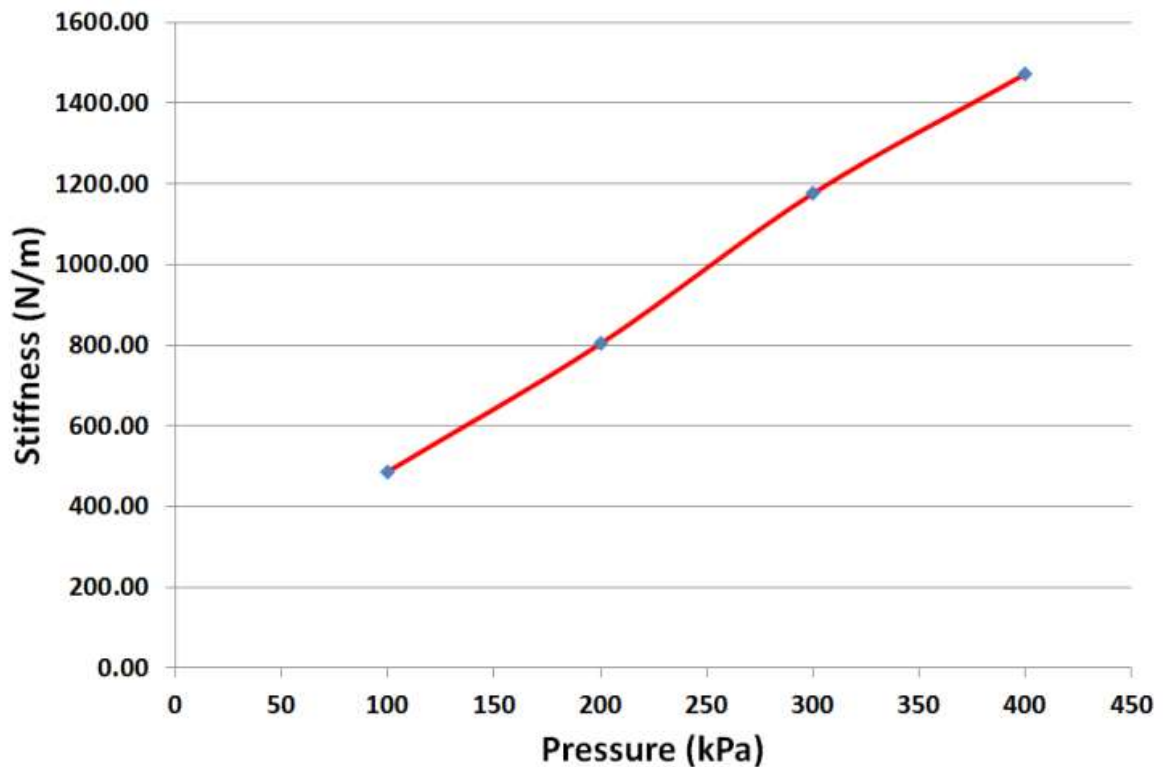


Figure 6. The extensor muscle stiffness in relation with increasing the supplied pressure.

It is obvious from the above plots that the contraction muscle has greater stiffness than the extensor. This is not an unexpected finding as although both actuators are constructed from the same braid and therefore have the same force/pressure profile the extensor muscle is able to displace almost double the distance of the contractor muscle. This means the gradient of a force/displacement plot for the extensor muscle would be considerably shallower than for the contractor muscle.

4. Novel Extensor-Contractor Pneumatic Artificial Muscles (ECPAM)

Based on the previous research presented in the literature review and the results presented above there are limitations associated with both the contraction and extensor muscles. These limitations are summarised as follows:

- The contraction muscle only generates a contraction force in response to supplied air pressure [18, 28].
- The extensor muscle only generates extension force in response to supplied air pressure [17, 18, 28, 29].
- There is no single PAM capable of performing both contraction (decreasing in length) and extension (increasing in length) with reference to its nominal length [30, 31].
- There is no single PAM able to produce bidirectional (extension and contraction) force [30, 32].
- Each muscle type has a fixed stiffness at a specific length and load [30, 32, 33].
- When muscle pressure is low (e.g. when the force the muscle is generating is small) actuator stiffness will be low as stiffness increases with pressure [32, 33].

These limitations inspired the design and construction of a novel Extensor-Contractor Pneumatic Artificial Muscles (ECPAM) as described in the following sections.

Several ideas of combining extensor and contractor have been already reported in the previous research such as [34] and [28]. These papers describe systems where the actuators are parallel to each other not one inside the other and our system is more compact and takes up less space. In addition, the force a muscle produces is a function of the surface area of the muscle not the volume. This means that the central volume of the muscle is “dead space” which must be pressurised but does not contribute to actuator force. Placing the contractor muscle inside the extensor muscle helps to fill this “dead space” meaning that the new actuator will use slightly less air than two muscles positioned side by side.

4.1. Design and Construction of the ECPAM

The Extensor-Contractor Pneumatic Artificial Muscle (ECPAM) is formed from a combination of contraction and extensor muscles. The new actuator consists of a contraction muscle placed inside an extensor muscle. The construction of the new actuator began with the creation of two end caps as shown in Figure 7 (a), these endcaps form the ends of both the extensor and contractor muscles. The thin central section of the endcaps is for attaching the contraction muscle and one of them has a hole in the centre for the air supply. The larger diameter section of the endcaps is for the outer extensor muscle and again one cap contains a hole in the side as shown in the Figure for the application of air.

As can be seen in Figure 7 (b) the contraction muscle is secured to the inner section of the two endcaps using a combination of nylon threads and a resin adhesive and then the muscle is inserted into the rubber bladder of the extensor muscle. The rubber bladder of the extension muscle is 15% shorter than the contraction muscle. The contraction muscle is therefore compressed inside extensor muscle’s bladder so that the bladder can be secured to the second endcap. The extensor muscle’s braided sleeve is then compressed and secured to the two endcap using both thread and plastic cable ties, as can be seen in Figure 7 (c).



Figure 7. Construction and operation of the novel ECPAM; (a) Endcaps design, (b) The contraction muscle inside the extensor muscle bladder, (c) The ECPAM with no pressure, (d) The ECPAM with pressurised only the inner contraction muscle by 300kPa, and (e) The ECPAM with pressurised only the outer extensor muscle by 200kPa.

Figure 7 (d) shows contraction of the ECPAM caused by pressurising the inner contraction muscle to 300kPa whilst the extensor muscle remains unpressurised. The extension operation of the actuator is illustrated in Figure 7(e) where the outer extensor muscle is pressurised to 200kPa whilst the contractor muscle remains unpressurised.

To investigate the relation between the supplied pressure and the muscle length an experiment was performed that involved inflating each muscle (the contractor and the extensor) independently gradually from zero to 500kPa in steps of 50kPa; the results are shown in Figure 8.

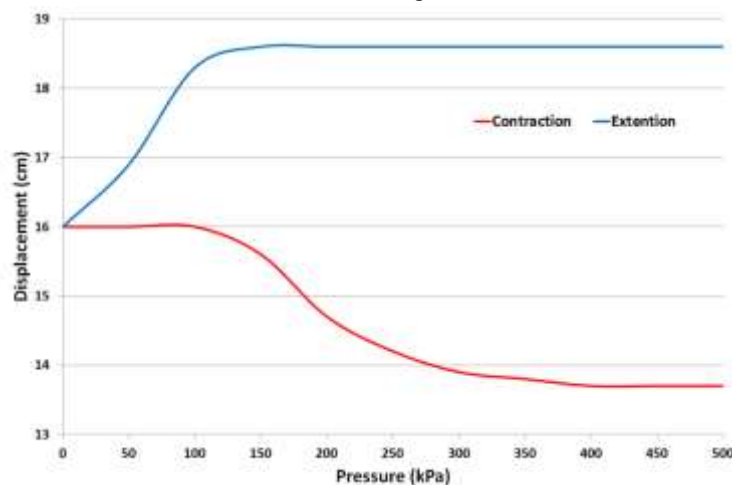


Figure 8. The experimental results of the relation between the ECPAM and increasing the supplied pressure for the inner and outer muscles independently.

The resting, unpressurised, length of the extensor muscle was 16cm. However, the contractor muscle was 15% longer than this which meant that when the ECPAM was unpressurised the contractor muscle would be compressed inside the bladder of the extensor muscle to a length of 16cm. As the extensor muscle was pressurised and extended the contractor muscle would become stretched until it reached its maximum length. At this point the contractor muscle would prevent the extensor muscle from being able to extend any further. From its resting length of 16cm to the point where the contractor muscle prevented any further extension of the ECPAM it extended by approximately 15% to 18.4cm, as can be seen in Figure 8.

As was proven previously the contractor muscle is able to contract by approximately 30%. This means that at its minimum length the contractor muscle would be shorter than the resting (unpressurised) length of the extensor muscle and this caused the extensor muscle to become compressed. Pressurising the contractor muscle to its maximum pressure whilst the extensor muscle was unpressurised resulted in the ECPAM contracting from its resting length of 16cm to 13.6cm, a contraction of approximately 15%, as can be seen in Figure 8. The overall ECPAM is therefore able to extend and contract from its resting length by approximately 15%.

4.2. Kinematics Analysis of ECPAM

Figure 9 illustrates the general geometry of PAM, assuming the middle part of the actuator is perfectly cylindrical and the actuator length L , Diameter D and θ represents the braid angle between a single braided thread and the muscle central axis [35]. The single thread of the sleeve b encircles the muscle n times.

The extensor actuator differs from the contractor in that the resting length of the sleeve is significantly longer than the length of the rubber tube. In other words, the sleeve must be compressed (θ increased) to reach the same length as the rubber tube.

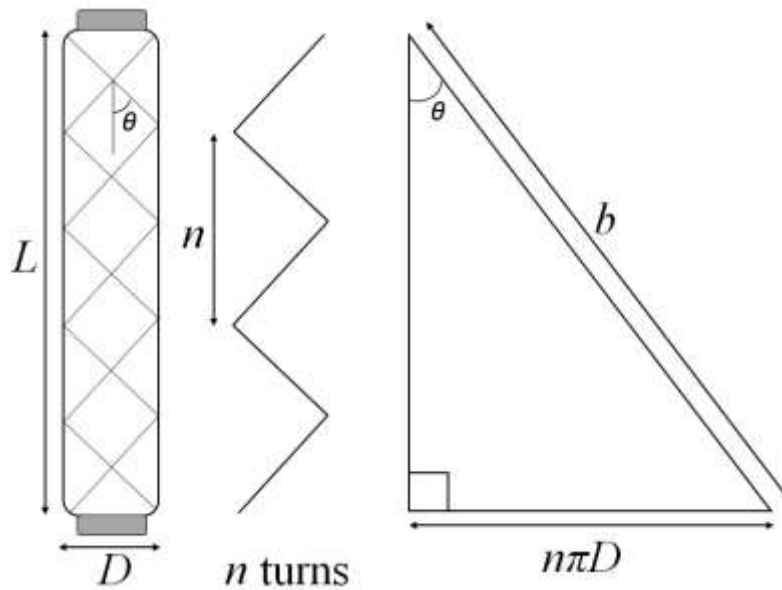


Figure 9. The general geometry of PAM.

Based on Figure 9 the initial length of the PAM will be:

$$L = b \cos \theta \quad (1)$$

And the muscle diameter:

$$D = \frac{b \sin \theta}{n\pi} \quad (2)$$

Assuming the middle segment of the PAM is cylinder then the actuator volume is:

$$V = \frac{\pi D^2 L}{4} \quad (3)$$

The analysis of the ECPAM is based on the following assumption: there are no friction forces between the braids and the bladders, or between the nylon threads of the braid, or between the contractor muscle and the bladder of the extensor muscle, and there are no elastic forces within the bladders. Figure 10 illustrates the geometrical kinematic analysis of the ECPAM.

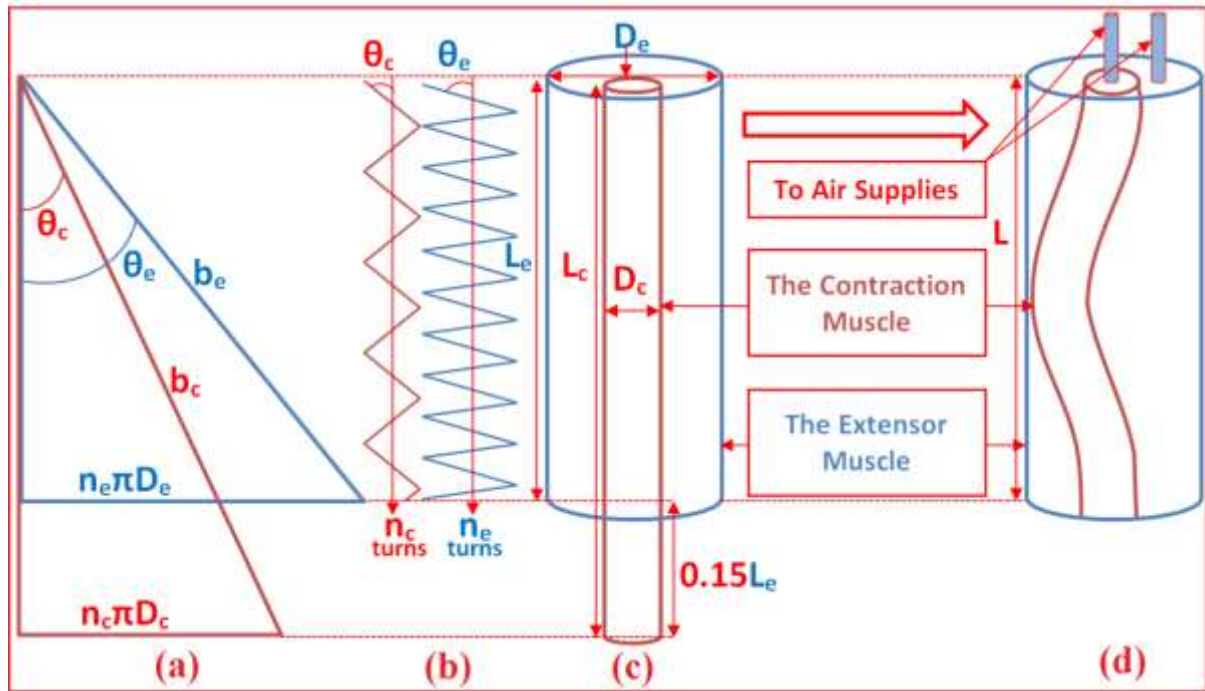


Figure 10. Kinematics of the ECPAM; (a) The general geometry of PAM (The contractor and the extensor muscles), (b) The braid angles and the number of turns of both muscles, (c) The lengths relation between the muscles and (c) The ECPAM design.

The ECPAM is constructed using the same contraction and extensor muscles (discussed above in sections 2 and 3). There is a geometrical relationship between these two muscles as follows: the resting sleeve diameter of the contraction muscle is half of the resting sleeve diameter of the extensor (both have the same sleeve type). As mentioned above, the contraction muscle is longer than the extensor muscle by 15% as shown in Figure 10 (c). Therefore at the resting length of the ECPAM the contraction muscle will be bent or compressed inside the extensor muscle to match the extensor muscle's length as shown in Figure 10 (d).

$$L_c = 1.15L_e \rightarrow L_e = \frac{1}{1.15}L_c \quad (4)$$

Where L_c is the contraction muscle length and L_e is extensor muscle length.

The sleeve length of the extensor muscle is double its bladder length (the ECPAM's resting length). From this and the sleeves resting diameter:

$$n_c = 1.15n_e \rightarrow n_e = \frac{1}{1.15}n_c \quad (5)$$

$$2b_c = 1.15b_e \rightarrow b_e = \frac{2}{1.15}b_c \quad (6)$$

Where n_c is the number of turns of thread in the contractor muscle, n_e is the number of turns of thread in the extensor muscle, b_c is the single thread length of the contraction muscle sleeve and b_e is the single thread length of the extensor muscle sleeve.

Based on Figure 10, the contraction and extensor muscles geometrical parameters will be:

$$L_c = b_c \cos \theta_c \quad (7)$$

$$L_e = b_e \cos \theta_e \quad (8)$$

$$D_c = \frac{b_c \sin \theta_c}{n_c \pi} \quad (9)$$

$$D_e = \frac{b_e \sin \theta_e}{n_e \pi} \quad (10)$$

$$V_c = \frac{\pi D_c^2 L_c}{4} \quad (11)$$

$$V_e = \frac{\pi D_e^2 L_e}{4} \quad (12)$$

Where θ_c is the angle between the braided thread and central actuator axis of the contraction muscle, θ_e is the angle between braid and central actuator axis of the extensor muscle, D_c is the contraction muscle diameter, D_e is the extensor muscle diameter, V_c is the contraction muscle volume and V_e is the extensor muscle volume.

4.3. Modelling the Output Force of the ECPAM

Chou et al. [35] derived the output force mathematical model of the PAM based on its cylindrical shape as follows:

$$F = -P' \frac{dV}{dL} \quad (13)$$

Where P' is the relative PAM pressure.

In the case of ECPAM's contraction muscle, the relative pressure in it is affected by the pressure inside the extensor muscle (i.e. a higher pressure in the extensor muscle reduces the relative pressure in the contractor muscle), therefore:

$$P' = (P_c - P_e) \quad (14)$$

where P_c is the pressure of the contraction muscle and P_e is the pressure of the extensor muscle.

Substituting equations (7), (11) and (14) into equation (13) gives the contraction muscle force F_c :

$$F_c = -(P_c - P_e) \frac{dV_c}{dL_c} \quad (15)$$

Differentiating equation (15) with respect to θ_c gives

$$F_c = \frac{b_c^2 (P_c - P_e)}{4\pi n_c^2} (3 \cos^2 \theta_c - 1) \quad (16)$$

The extensor muscle is affected by the volume of the contraction muscle, in effect the contractor muscle represents a hollow cylindrical section along the centre of the extensor muscle. This means the true shape of the extensor muscle is represented by a thick wall cylindrical shell, therefore the cylinder extensor muscle force F_s will be:

$$F_s = P_e \frac{dV_s}{dL_e} = P_e \frac{dV_e - dV_c}{dL_e} = P_e \left(\frac{dV_e}{dL_e} - \frac{dV_c}{dL_e} \right) \quad (17)$$

Where V_s is the volume of the cylinder representing the extensor muscle.

By substituting the relation between the contractor and extensor muscles lengths in equation (4) into equation (17):

$$F_s = P_e \left(\frac{dV_e}{dL_e} - 1.15 \frac{dV_c}{dL_c} \right) \quad (18)$$

Differentiating equation (18) gives:

$$F_s = P_e \left(\frac{dV_e/d\theta_e}{dL_e/d\theta_e} - 1.15 \frac{dV_c/d\theta_c}{dL_c/d\theta_c} \right) = P_e \left(1.15 \frac{b_c^2(3 \cos^2 \theta_c - 1)}{4\pi n_c^2} - \frac{b_e^2(3 \cos^2 \theta_e - 1)}{4\pi n_e^2} \right) \quad (19)$$

Substituting equations (5) and (6) into equation (19) and simplifying the result gives:

$$F_s = \frac{b_e^2 P_e}{4\pi n_e^2} (1.15(3 \cos^2 \theta_c - 1) - 4(3 \cos^2 \theta_e - 1)) \quad (20)$$

The ECPAM has two opposite forces: F_c is the contraction force and F_s is the extension force.

$$F = (F_c - F_s) \begin{cases} \text{if } F \text{ is positive} \rightarrow \text{it is a Contraction Force} \\ \text{if } F \text{ is negative} \rightarrow \text{it is a Extension Force} \end{cases}$$

(21)

Substituting equations (16) and (20) in equation (21) and simplifying the result gives the ECPAM total force model F :

$$F = \frac{b_c^2}{4\pi n_c^2} (P_c(3 \cos^2 \theta_c - 1) + 0.15P_e(3 \cos^2 \theta_c - 1) - P_e(3 \cos^2 \theta_e - 1)) \quad (22)$$

4.4. Experimental Verification of the ECPAM Output Force Model

An experimental verification of the ECPAM model has been performed using the experimental setup shown in Figure 11. The ECPAM was suspended vertically in a rig with the unpressurised actuator being at its resting length (16cm). The end cap through which air was supplied was secured to a mounting plate and the free end of the actuator was attached via a load cell to a second fixed point. The actuator was surrounded by a rigid cylindrical nylon tube to limit the any buckling or lateral deformations of the muscle during extension force testing, as shown in Figure 11 (b) and (c). Figure 11 (a) illustrates how the contraction force could be measured using the same rig by reversing the load cell direction and removing the cylinder tube.

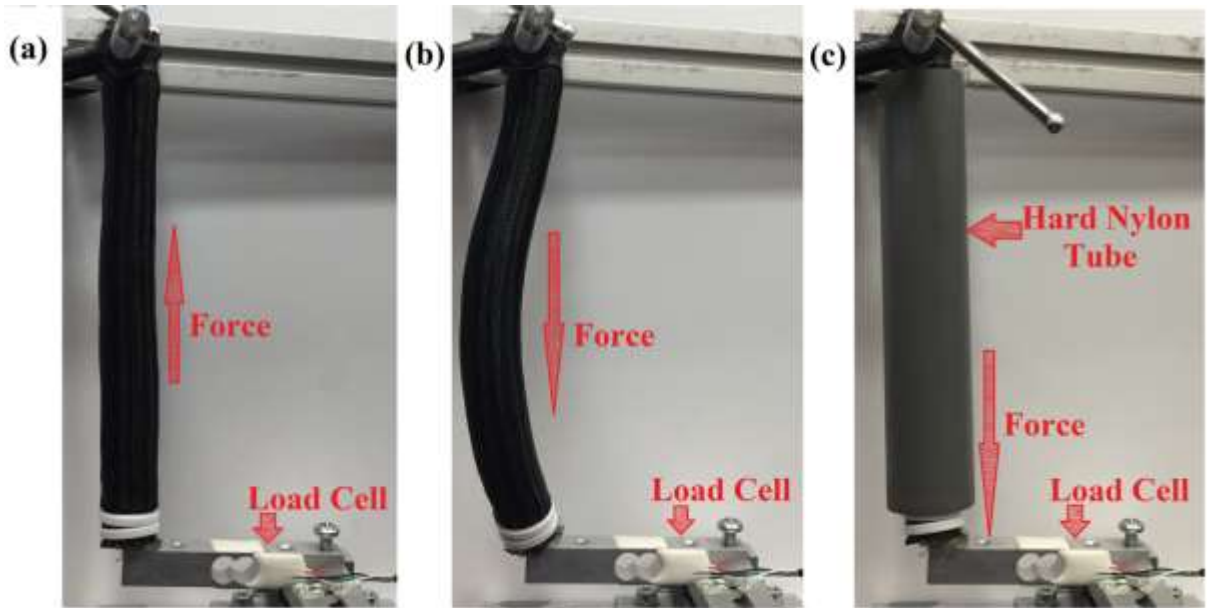


Figure 11. Experiment setup to calculate the extension and contraction force of the ECPAM; (a) Calculating the contraction force of the ECPAM, (b) Buckling or lateral deformations of the ECPAM at extension and (c) Calculating the extension force of the ECPAM with a rigid cylindrical nylon tube.

The experiment began by pressurising the extensor muscle to 100kPa (P_e) and recording the extension force measured by the load cell. The pressure in the contraction muscle (P_c) was then gradually increased from zero to 500kPa in 50kPa increments and the contraction force was recorded. The experiment was then repeated twice more with the extensor muscle pressure (P_e) equal to 300kPa and 500kPa. Figure 12 shows the experimental results of these three experiments.

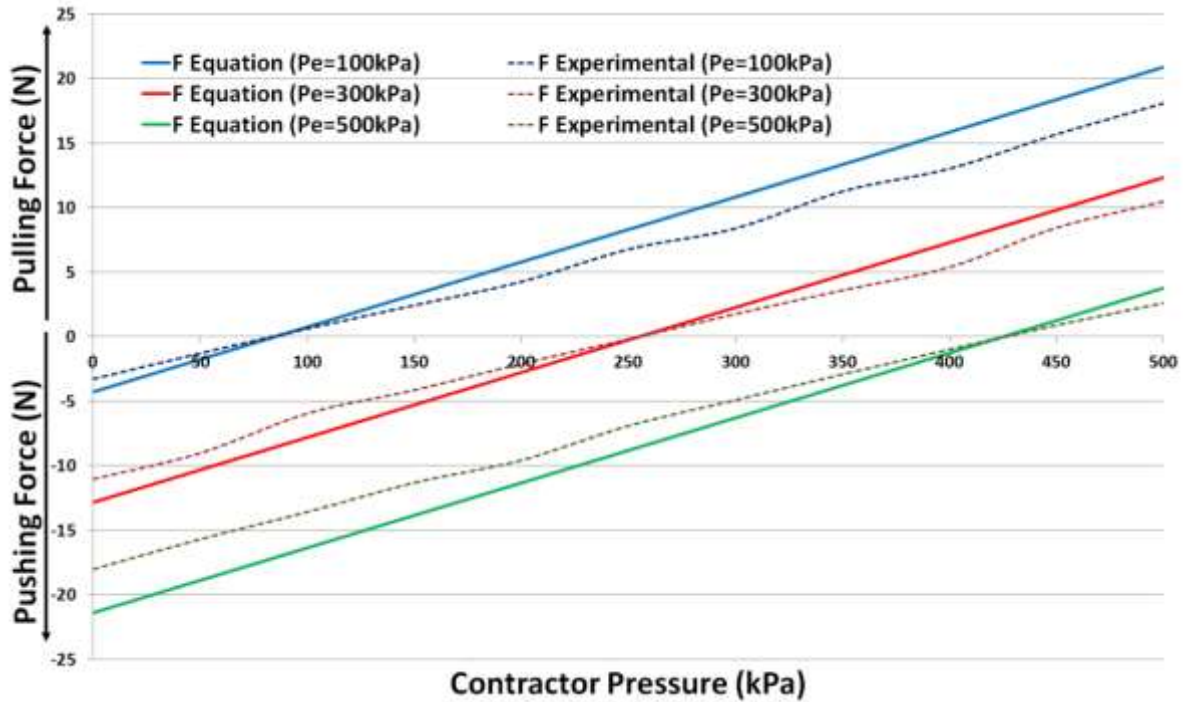


Figure 12. The Experimental results of the output force of the ECPAM with its mathematical model (the upper part of the graph shows the contraction forces and the lower part shows the extension forces of the ECPAM).

The average error percentages between the mathematical model and the experimental results are 20.23%, 20.31% and 21.09% for the three experiments with extensor muscle pressures 100kPa, 300kPa and 500kPa respectively. These errors were expected because the force losses were neglected; for example we assumed there were no frictional forces between the braids and the bladders or between the nylon threads of the braid or between the contractor muscle and the bladder of the extensor muscle and that there were no elastic forces within the bladders.

These losses caused these errors as an approximately fixed percentage (20%) of the total force and this increased in relation with the force. Based on this a correction factor C is introduced to represent these losses and decrease the average error percentage as far as possible. A similar approach has been used by other researchers to account for frictional losses and hysteresis in the past [28]. The total force equation with the suggested correction factor will be:

$$F_t = F - CF \quad (23)$$

This correction factor was calculated experimentally and in this work was assumed it to be 20%, derived from the average error percentage between the experimental results and our mathematical model. Figure 13 shows the new mathematical force model with consideration of the correction factor and the experimental results.

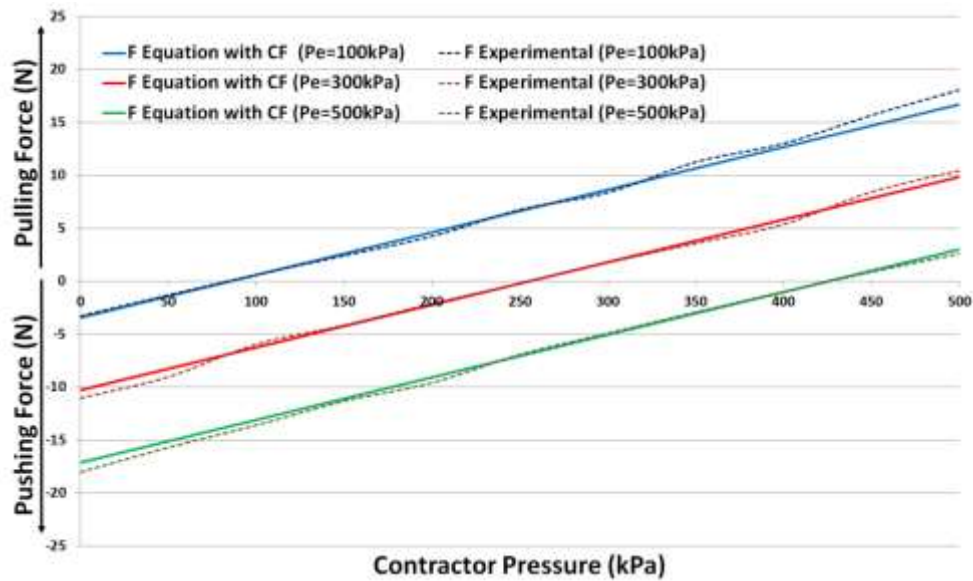


Figure 13. The Experimental results of the output force of the ECPAM with its mathematical model with consideration of correction factor (the upper part of the graph shows the contraction forces and the lower part shows the extension forces of the ECPAM).

The average error percentages between the mathematical model, with the correction factor, and the experimental results are 5.32%, 5.91% and 5.14% for the three experiments with extensor muscle pressures 100kPa, 300kPa and 500kPa respectively. Clearly more advanced mathematical models of the actuator performance would reduce the need for the correction factor and more detailed modelling of the new actuator will represent future work.

As can be seen in the experimental procedure buckling of the actuator was a potential problem and a mechanical support was used to prevent it. In the new actuator both the internal contractor muscle and the external extensor can experience buckling. However, in reality buckling of contractor muscle only occurs when it is unpressurised and so has effect on the force output of the actuator, as soon as the contractor is pressurised it will experience tension and this will force it into a straight, unbuckled configuration. Buckling of the extensor muscle is more of a problem. When the extensor muscle extends it places the contractor muscle inside it under tension, which causes it to behave like an internal tether between the two endcaps. If the extensor muscle buckles it makes contact with the taught contractor muscle which prevents it from extreme buckling, however, some degree of buckling is still possible. This is a problem common to many types of soft extending pneumatic actuator not just the new actuator described in this paper. There are various methods that can be used to prevent buckling of extending actuators including the addition of a rigid support structure or soft guides located on the mechanical structure being actuated which prevent buckling. Alternative methods include using the muscle as a bending actuator (i.e. intentionally creating and exploiting buckling) or as part of a continuum manipulator. These methods will be further explored as future work on the application of the new actuator.

5. Stiffness of the ECPAM

At a fixed load and position a traditional pneumatic muscle has a single fixed stiffness value. The reason for this is that the actuator's stiffness is a result of the pressure in the actuator, with higher pressure resulting in greater stiffness. However, pressure is proportional to muscle output force and so increasing the pressure in a muscle which is supporting a fixed load will result in contraction of the muscle and an change in position. It is therefore not possible to change a pneumatic muscle's stiffness independently of its force or position. The newly developed ECPAM, however, has the ability to potentially vary its stiffness independently of its position.

Stiffness experiments were conducted to prove and validate that the novel ECPAM's stiffness can be adjusted without resulting in a change of actuator length. The ECPAM was again suspended vertically, but this time with the distal end being free. The actuator was initially at its unpressurised nominal length of 16cm. The

contractor muscle was pressurised to 100kPa which resulted in a shortening with reference to the nominal length. The pressure in the extensor muscle was then increased until the actuator extended in length to again reach the nominal length. That extensor pressure required to achieve this was measured to be 75kPa. To calculate the stiffness at this combination of muscle pressures, loads of increasing mass were applied to the free end of the muscle and the axial displacement at each load was measured. It was then possible to determine the stiffness from the gradient of the resultant force/displacement plot Figure 14 and this was found to be 4611N/m. To prove that it was possible to achieve a different stiffness value at the same length, the contractor muscle pressure was increased to 150kPa. This again caused the ECPAM to become shorter than the nominal length and so the extensor muscle pressure was again increased until it reached its nominal length (16cm). The extensor pressure required to achieve this was 100kPa. The stiffness was again found experimentally and calculated to be 5478N/m. The reason the stiffness increased was because both the muscle pressures were higher and as previously stated stiffness is a function of muscle pressure. For further verification that the stiffness could be varied at a fixed length (16cm), the experiment was repeated twice more at the same actuator length but with the pressure in the contractor and extensor muscles being $P_c=200\text{kPa}/P_e=125\text{kPa}$ and $P_c=250\text{kPa}/P_e=150\text{kPa}$ respectively. The resulting stiffness values were determined to be 6172N/m and 7788N/m respectively. The experimental results from all four experiments are shown in Figure 14 and it can be seen that different stiffness can be achieved at the same actuator length.

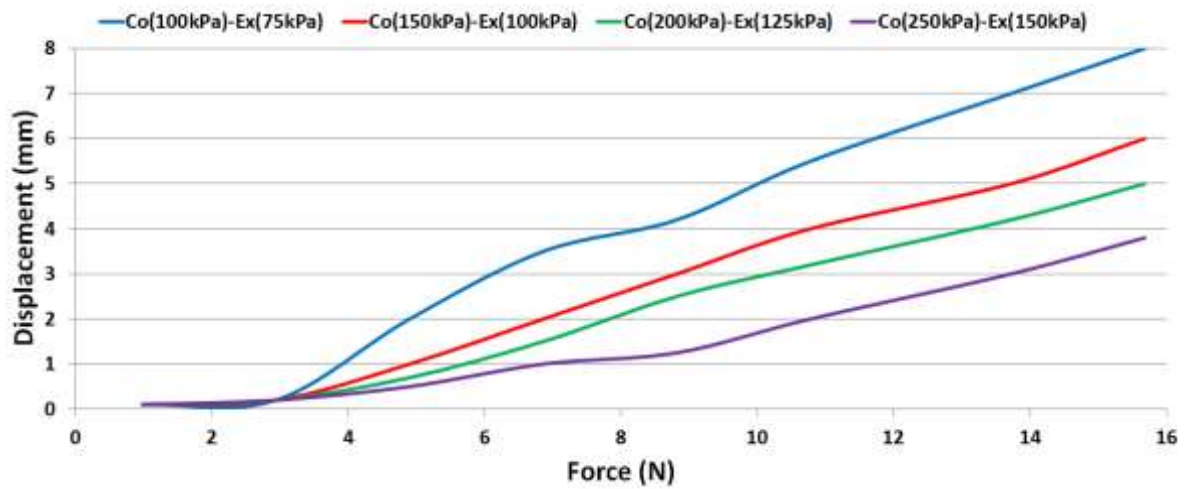


Figure 14. Stiffness experimental results for the ECPAM at length 16cm.

For further verification that the stiffness of the ECPAM can be adjusted whilst at a fixed length the same experiment described above was repeated twice more, once with a muscle length shorter than the nominal length (15cm) and once with it longer (17cm). All ECPAM's stiffness results are summarised in Table 2.

Table 2. A summary of ECPAM's stiffness results.

Experiment No.	Muscle Length	P_c	P_e	Stiffness
1	16cm	100kPa	75kPa	4611N/m
2	16cm	150kPa	100kPa	5478N/m
3	16cm	200kPa	125kPa	6172N/m
4	16cm	250kPa	150kPa	7788N/m
5	15cm	200kPa	60kPa	3550N/m
6	15cm	250kPa	90kPa	5796N/m
7	15cm	300kPa	120kPa	7492N/m
8	15cm	350kPa	150kPa	9961N/m
9	17cm	50kPa	100kPa	1634N/m
10	17cm	100kPa	125kPa	2640N/m
11	17cm	150kPa	150kPa	3077N/m
12	17cm	200kPa	175kPa	5337N/m

Unlike a traditional pneumatic muscle, the ECPAM can have the same stiffness at different lengths. In the table above it can be seen that experiments 2,6 and 12 all have broadly similar stiffness values but in each the muscle length is different. This therefore proves that ECPAM's stiffness can be set independently of position (actuator length).

6. Stiffness and Position (length) Control of the ECPAM

Accurate control of McKibben muscles presents a major challenge, this is because of both the nonlinear behaviour of the muscles and the compressibility of air. Much of the control of pneumatic muscle has relied on classical control techniques and simple models of the actuator functionality that include many assumptions.

Based on the above experimental stiffness results a control system has been created capable of controlling both the length and the stiffness of the novel ECPAM, as shown in Figure 15. The first stage of the stiffness and position controller system is a neural network identifier. This stage is utilized to generate the appropriate pressures set-point for the contractor and extensor muscles, based on our stiffness experiments in Table 2. This neural network identifier is designed using a Matlab neural network data fitting application (one of the curve fitting techniques based on inputs and its outputs data). The experimental stiffness and lengths data for the ECPAM are used as inputs and the amount of appropriate contractor and extensor pressures are utilised as outputs to design this identifier. This neural network includes one input layer, four two layers and one output layer. A Bayesian Regularization [36] training technique is used to train the proposed neural network identifier. It is a network training technique that updates the weight and bias values according to Levenberg-Marquardt optimization; it minimizes a combination of squared errors and weights, and then determines the correct combination so as to produce a network that generalizes well.

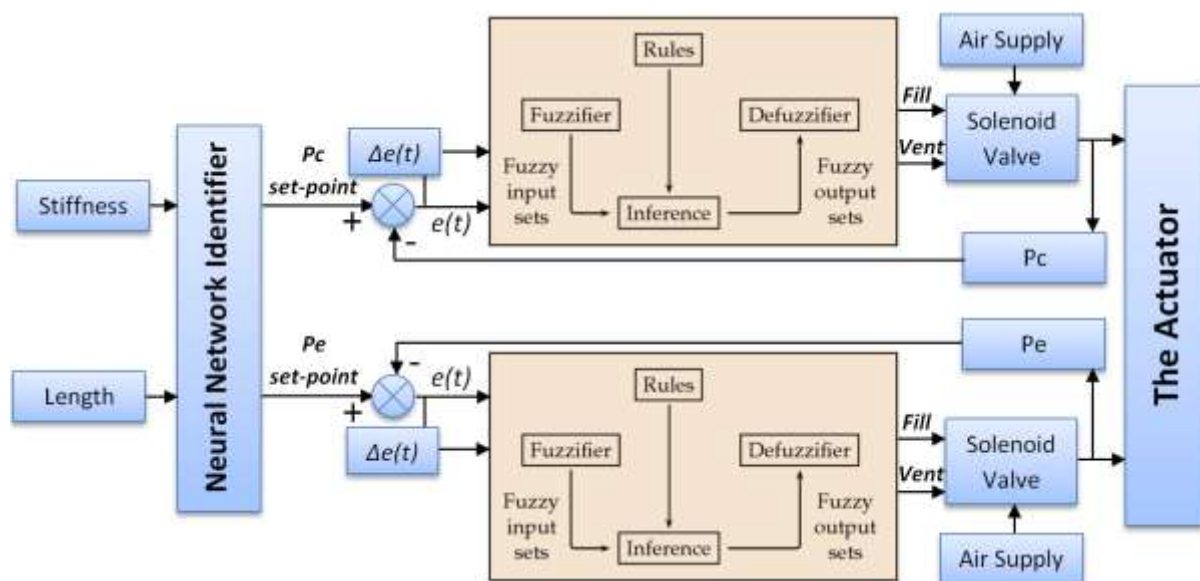


Figure 15. The proposed stiffness and position controller of the ECPAM.

Two Fuzzy logic controllers are utilised in the stiffness-position controller system to control the level of pressure inside the contractor and extensor muscles. The appropriate pressure set-points for each contractor and extensor muscle come from the neural network identifier. These two fuzzy controllers are identical. Each one has two inputs (error and change of error) and two outputs (Fill and Vent). MATRIX 3x3 solenoid valves are used to control the air flow by PWM (Pulse Width Modulation); the same valve port can be used as either a fill or vent valve depending on the applied PWM signal. The ECPAM has two valves, one for the contractor muscle and the other for the extensor muscle. The feedback pressures is calculated by MDPS002 pressure sensor (700kPa) vacuum absolute pressure sensor. Based on this, each Fuzzy controller has two outputs to control the

percentage of the PWM duty cycle for each filling and venting valve. The valve PWM frequency is 125Hz. Figure 16 shows the membership functions of the inputs and outputs of both Fuzzy controllers.

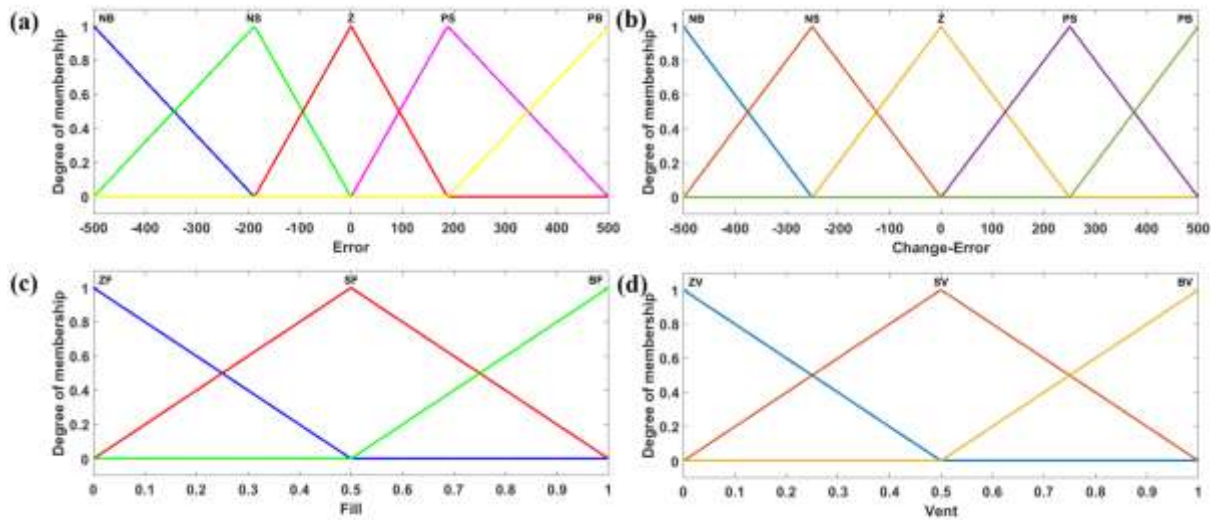


Figure 16. The membership functions for the inputs and outputs for the Fuzzy controllers of the proposed stiffness and position controller of the ECPAM; where NB is Negative Big, NS is Negative Small, Z is Zero, PS is Positive Small, PB is Positive Big, ZF is Zero Fill, SF is Small Fill, BF is Big Fill, ZV is Zero Vent, SV is Small Vent and BV is Big Vent; (a) The membership function of the input error, (b) The membership function of the input change in error, (c) The membership function of the Fill output and (d) The membership function of the Vent output.

There are five ranges for the input error and five ranges for the change in error, with the entire range being -500 to 500, because the contractor and the extensor muscles act in a range between zero to 500kPa; this range of pressure was chosen based on the maximum operating pressures of the valves. Likewise, there are three intervals for PWM fill output percentage and the same for vent output. All membership functions are triangle type for its straightforwardness, but the membership functions of the error input are smaller close intervals to zero. This serves to diminish the gain of the controller close to the desired set point, to achieve superior stability and to avoid excessive overshoots on the controller response. Figure 17 demonstrates the Fuzzy controllers rules surface of each fill and vent output.

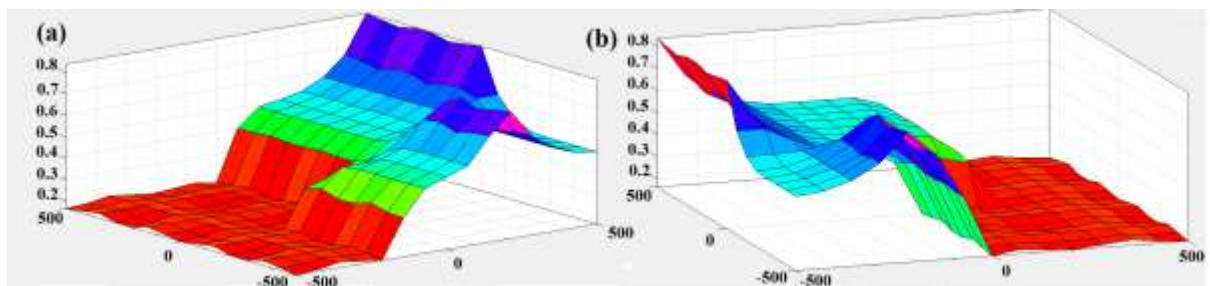


Figure 17. The Fuzzy controllers rules surfaces of each Fill and Vent outputs; (a) The rules surface of the Fill output and (b) The rules surface of the Vent output.

The proposed stiffness-position controller was experimentally tested. Six different experiments were conducted to examine the performance of the proposed control system, as shown in Figures 22, 23 and 24. Figure 18 illustrates two experimental results. The first experiment in Figure 18 (a) was with a stiffness set point of 7500N/m and an actuator length of 15cm. At these stiffness and length set points, the neural network identifier generated contractor and extensor pressures of 300.6kPa and 119.8kPa respectively. The second experiment in Figure 18 (b) was with a stiffness set point of 3500N/m and the same actuator length 15cm. At these stiffness and length set points, the neural network identifier generated contractor and extensor pressures of 199.1kPa and 59.78kPa respectively. These two experiments prove that we can control the stiffness of our novel actuator without changing its length.

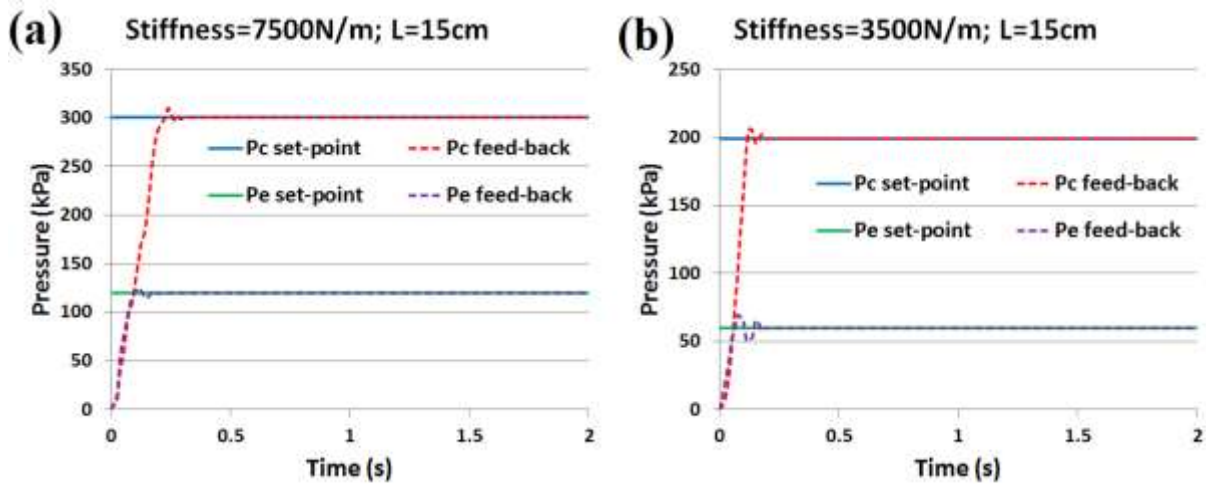


Figure 18. Stiffness-position controller results at actuator length 15cm and two different stiffness.

To validate this concept, we conducted another two experiments for another actuator length as shown in Figure 19. The first experiment in Figure 19 (a) was with a stiffness set point of 6000N/m (randomly chosen) and actuator length of 16cm. The identifier in this case generated contractor and extensor pressures of 186.6kPa and 117.5kPa respectively. The second experiment in Figure 19 (b) was with a stiffness set point of 4500N/m and the same actuator length 16cm. At these stiffness and length set points, the neural network identifier generated contractor and extensor pressures of 92.44kPa and 72.14kPa respectively.

For further validation, we also conducted another two experiments for another actuator length as shown in Figure 20. The first experiment in Figure 20 (a) was with a stiffness set point of 5000N/m (randomly chosen) and actuator length of 17cm. The identifier in this case generated contractor and extensor pressures of 192kPa and 170.4kPa respectively. The second experiment in Figure 20 (b) was with a stiffness set point of 2500N/m and the same actuator length 17cm. At these stiffness and length set points, the neural network identifier generated contractor and extensor pressures of 92.66kPa and 120.8kPa respectively.

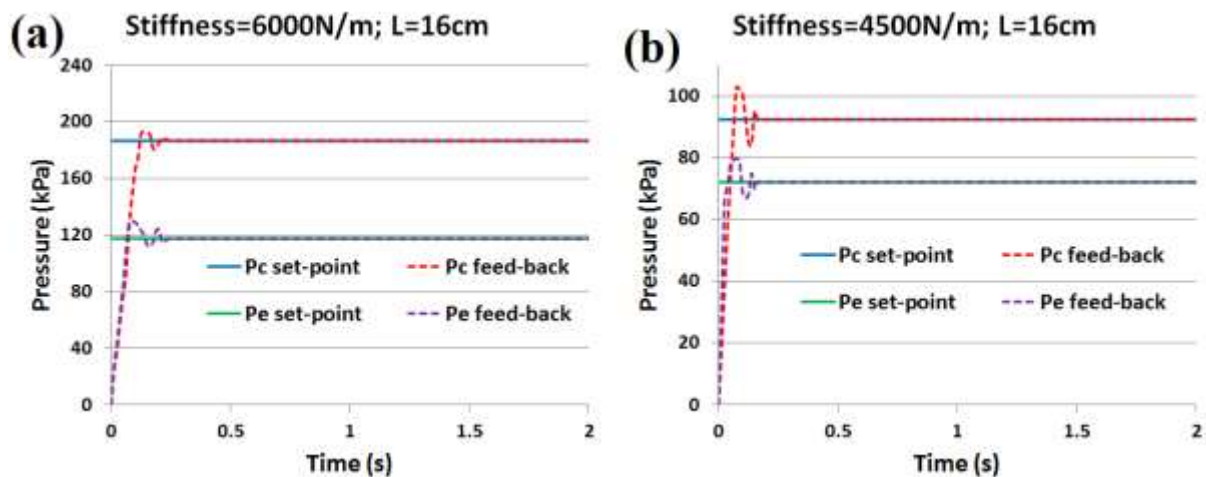


Figure 19. Stiffness-position controller results at actuator length 16cm and two different stiffness values.

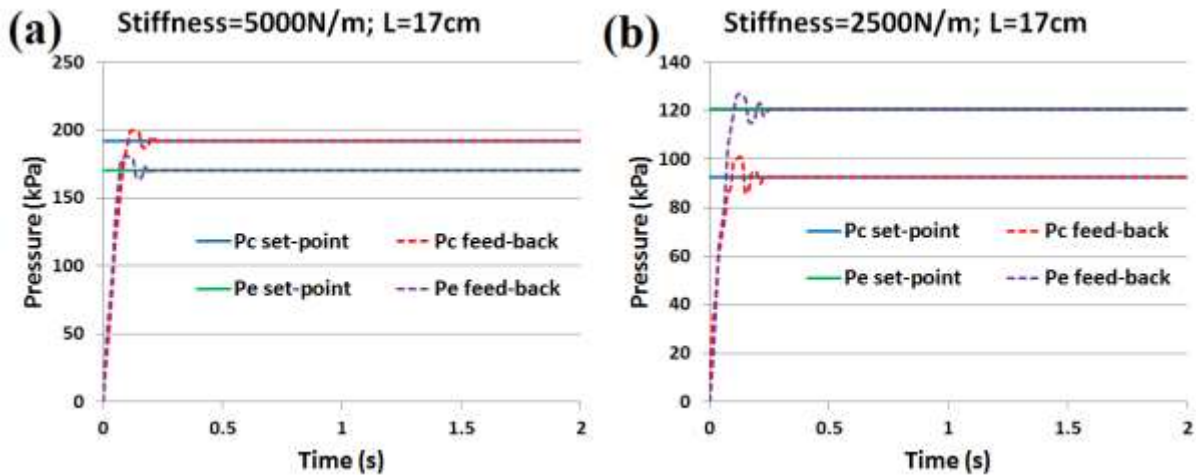


Figure 20. Stiffness-position controller results at actuator length 17cm and two different stiffness values.

The actuator length and stiffness results of all of the above six experiments in Figures 22, 23 and 24 were verified manually after each experiment. The length was measured and the stiffness determined using the same experimental procedure described in section 5. The average percentage error of the ECPAM stiffness and length were determined to be 3.95% and 4.18% respectively.

7. Conclusions

This paper has described the design and construction of a novel extensor-contractor pneumatic muscle. This new actuator overcomes some of the limitations associated with the use of single pneumatic muscles as well as having additional features. This new actuator has bidirectional action allowing it to both extend and contract and create force in both directions.

A mathematical model has been developed for the new novel ECPAM which describes the actuator output force. This mathematical model has been verified experimentally with the average error percentage between the mathematical model and the experimental results being less than 6%.

The stiffness of a pneumatic muscle is dependent on the pressure inside it, however, for a fixed load the length of a traditional pneumatic muscle is also a function of pressure. This means that it is not possible to change the stiffness of a pneumatic muscle (with a fixed load) without changing its length. It has been shown that the new ECPAM is able to adjust its stiffness without this resulting in a change of actuator length. Numerous stiffness and length experiments were performed to investigate the ability to vary the actuator's stiffness independently of position. A stiffness position controller has been developed to control the stiffness of the actuator at specific lengths. Verification was conducted using the controller and the average stiffness and position errors were found to be less than 5%.

Future work will seek to improve the mathematical model further by considering other losses such as rubber bladder impedance, the friction between the bladder and the braided sleeve, and the friction between the fibre threads in the braid. This will be done to enhance the mathematical model and decrease the average percentage error.

References

- [1] D. Trivedi, C. D. Rahn, W. M. Kier, and I. D. Walker, "Soft robotics: Biological inspiration, state of the art, and future research," *Applied Bionics and Biomechanics*, vol. 5, pp. 99-117, 2008.
- [2] J. E. Takosoglu, P. A. Laski, S. Blasiak, G. Bracha, and D. Pietrala, "Determining the static characteristics of pneumatic muscles," *Measurement and Control*, vol. 49, pp. 62-71, 2016.
- [3] Y. Cui, T. Matsubara, and K. Sugimoto, "Pneumatic artificial muscle-driven robot control using local update reinforcement learning," *Advanced Robotics*, vol. 31, pp. 397-412, 2017.
- [4] M. D. Doumit and S. Pardoel, "Dynamic contraction behaviour of pneumatic artificial muscle," *Mechanical Systems and Signal Processing*, vol. 91, pp. 93-110, 2017.

- [5] N. N. Son, C. Van Kien, and H. P. H. Anh, "A novel adaptive feed-forward-PID controller of a SCARA parallel robot using pneumatic artificial muscle actuator based on neural network and modified differential evolution algorithm," *Robotics and Autonomous Systems*, vol. 96, pp. 65-80, 2017.
- [6] J. D. Greer, T. K. Morimoto, A. M. Okamura, and E. W. Hawkes, "Series pneumatic artificial muscles (sPAMs) and application to a soft continuum robot," in *Robotics and Automation (ICRA), 2017 IEEE International Conference on*, 2017, pp. 5503-5510.
- [7] T. Tang, S. Chong, M. Tan, C. Chan, and K. Sato, "Characterization of Pneumatic Artificial Muscle System in an Opposing Pair Configuration," *Journal of Telecommunication, Electronic and Computer Engineering (JTEC)*, vol. 8, pp. 73-77, 2016.
- [8] G. Andrikopoulos, G. Nikolakopoulos, and S. Manesis, "Pneumatic artificial muscles: A switching Model Predictive Control approach," *Control Engineering Practice*, vol. 21, pp. 1653-1664, 2013.
- [9] G. Andrikopoulos, G. Nikolakopoulos, and S. Manesis, "Design and development of an exoskeletal wrist prototype via pneumatic artificial muscles," *Meccanica*, vol. 50, pp. 2709-2730, 2015.
- [10] D. Gryparis, G. Andrikopoulos, and S. Manesis, "Parallel robotic manipulation via Pneumatic Artificial Muscles," in *11th International Conference on Informatics in Control, Automation and Robotics (ICINCO), 2014* 2014, pp. 29-36.
- [11] N. Tsagarakis and D. G. Caldwell, "Improved modelling and assessment of pneumatic muscle actuators," in *IEEE International Conference on Robotics and Automation, 2000. Proceedings. ICRA'00.* , 2000, pp. 3641-3646.
- [12] J. Burgner-Kahrs, D. C. Rucker, and H. Choset, "Continuum robots for medical applications: A survey," *IEEE Transactions on Robotics*, vol. 31, pp. 1261-1280, 2015.
- [13] B.-S. Kang and E. J. Park, "Modeling and control of an intrinsic continuum robot actuated by pneumatic artificial muscles," in *Advanced Intelligent Mechatronics (AIM), 2016 IEEE International Conference on*, 2016, pp. 1157-1162.
- [14] R. Kang, Y. Guo, L. Chen, D. T. Branson III, and J. S. Dai, "Design of a pneumatic muscle based continuum robot with embedded tendons," *IEEE/ASME Transactions on Mechatronics*, vol. 22, pp. 751-761, 2017.
- [15] B. S. Kang, "Kinematics of an Intrinsic Continuum Robot with Pneumatic Artificial Muscles," *Transactions of the Korean Society of Mechanical Engineers A*, vol. 40, pp. 289-296, 2016.
- [16] M. Luo, E. H. Skorina, W. Tao, F. Chen, S. Ozel, Y. Sun, *et al.*, "Toward Modular Soft Robotics: Proprioceptive Curvature Sensing and Sliding-Mode Control of Soft Bidirectional Bending Modules," *Soft Robotics*, vol. 4, pp. 117-125, 2017.
- [17] H. Al-Fahaam, S. Davis, and S. Nefti-Meziani, "Power assistive and rehabilitation wearable robot based on pneumatic soft actuators," in *Methods and Models in Automation and Robotics (MMAR), 2016 21st International Conference on*, 2016, pp. 472-477.
- [18] H. Al-Fahaam, S. Davis, and S. Nefti-Meziani, "Wrist rehabilitation exoskeleton robot based on pneumatic soft actuators," in *Students on Applied Engineering (ICSAE), International Conference for*, 2016, pp. 491-496.
- [19] H. Zheng and X. Shen, "Double-acting sleeve muscle actuator for bio-robotic systems," in *Actuators*, 2013, pp. 129-144.
- [20] T. Hassan, M. Cianchetti, B. Mazzolai, C. Laschi, and P. Dario, "A multifunctional pneumatic artificial muscle. Proof of concept."
- [21] F. Daerden and D. Lefeber, "Pneumatic artificial muscles: actuators for robotics and automation," *European journal of mechanical and environmental engineering*, vol. 47, pp. 11-21, 2002.
- [22] T. E. Pillsbury, Q. Guan, and N. M. Wereley, "Comparison of contractile and extensile pneumatic artificial muscles," in *IEEE International Conference on Advanced Intelligent Mechatronics (AIM), 2016* 2016, pp. 94-99.

- [23] B. Tondu, "Modelling of the McKibben artificial muscle: A review," *Journal of Intelligent Material Systems and Structures*, vol. 23, pp. 225-253, 2012.
- [24] G. Andrikopoulos, G. Nikolakopoulos, and S. Manesis, "A survey on applications of pneumatic artificial muscles," in *19th Mediterranean Conference on Control & Automation (MED), 2011* 2011, pp. 1439-1446.
- [25] D. G. Caldwell, G. A. Medrano-Cerda, and M. Goodwin, "Control of pneumatic muscle actuators," *IEEE control systems*, vol. 15, pp. 40-48, 1995.
- [26] F. Daerden and D. Lefeber, "The concept and design of pleated pneumatic artificial muscles," *International Journal of Fluid Power*, vol. 2, pp. 41-50, 2001.
- [27] L. A. Al Abeach, S. Nefti-Meziani, and S. Davis, "Design of a variable stiffness soft dexterous gripper," *Soft Robotics*, 2017.
- [28] M. E. Giannaccini, C. Xiang, A. Atyabi, T. Theodoridis, S. Nefti-Meziani, and S. Davis, "Novel design of a soft lightweight pneumatic continuum robot arm with decoupled variable stiffness and positioning," *Soft robotics*, vol. 5, pp. 54-70, 2018.
- [29] H. Al-Fahaam, S. Davis, and S. Nefti-Meziani, "The design and mathematical modelling of novel extensor bending pneumatic artificial muscles (EBPAMs) for soft exoskeletons," *Robotics and Autonomous Systems*, vol. 99, pp. 63-74, 2018.
- [30] L. A. Al Abeach, S. Nefti-Meziani, and S. Davis, "Design of a variable stiffness soft dexterous gripper," *Soft robotics*, vol. 4, pp. 274-284, 2017.
- [31] W. Parandyk, M. Ludwicki, B. Zagrodny, and J. Awrejcewicz, "The Positioning of Systems Powered by McKibben Type Muscles," in *Mechatronics-Ideas for Industrial Application*, ed: Springer, 2015, pp. 133-140.
- [32] C. Xiang, M. E. Giannaccini, T. Theodoridis, L. Hao, S. Nefti-Meziani, and S. Davis, "Variable stiffness McKibben muscles with hydraulic and pneumatic operating modes," *Advanced Robotics*, vol. 30, pp. 889-899, 2016.
- [33] M. Doumit and J. Leclair, "Development and testing of stiffness model for pneumatic artificial muscle," *International Journal of Mechanical Sciences*, vol. 120, pp. 30-41, 2017.
- [34] K. Suzumori, S. Wakimoto, K. Miyoshi, and K. Iwata, "Long bending rubber mechanism combined contracting and extending fluidic actuators," in *Intelligent Robots and Systems (IROS), 2013 IEEE/RSJ International Conference on*, 2013, pp. 4454-4459.
- [35] C.-P. Chou and B. Hannaford, "Measurement and modeling of McKibben pneumatic artificial muscles," *IEEE Transactions on robotics and automation*, vol. 12, pp. 90-102, 1996.
- [36] H. B. Demuth, M. H. Beale, O. De Jess, and M. T. Hagan, *Neural network design*: Martin Hagan, 2014.